Electronic Supplementary Material (ESI) for Journal of Materials Chemistry C.

Supporting Information

Size-Responsive Phase Transition Mechanism and Upconversion/Downshifting Luminescence Property of $KLu_2F_7:Yb^{3+}/Er^{3+}$ Nanocrystals

Xia Xu,[a,b] Xuesong Zhai,[c] Kaimin Du,[a,d] Pengpeng Lei,[a,b] Lile Dong,[a,d] Ruiping Deng,[a] Jing Feng,[a] and Hongjie Zhang*[a]*

[a] State Key Laboratory of Rare Earth Resource Utilization, Changchun Institute of Applied Chemistry, Chinese Academy of Science, 5625 Renmin Street, Changchun 130022, China. E-mail: fengj@ciac.ac.cn; hongjie@ciac.ac.cn; Fax: +86-431-85698041; Tel: +86-431-85262127

[b] University of Chinese Academy of Sciences, Beijing 100049, China

[c] School of Materials Engineering, Yancheng Institute of Technology, Yancheng 224051, China

[d] University of Science and Technology of China, Hefei 230026, China

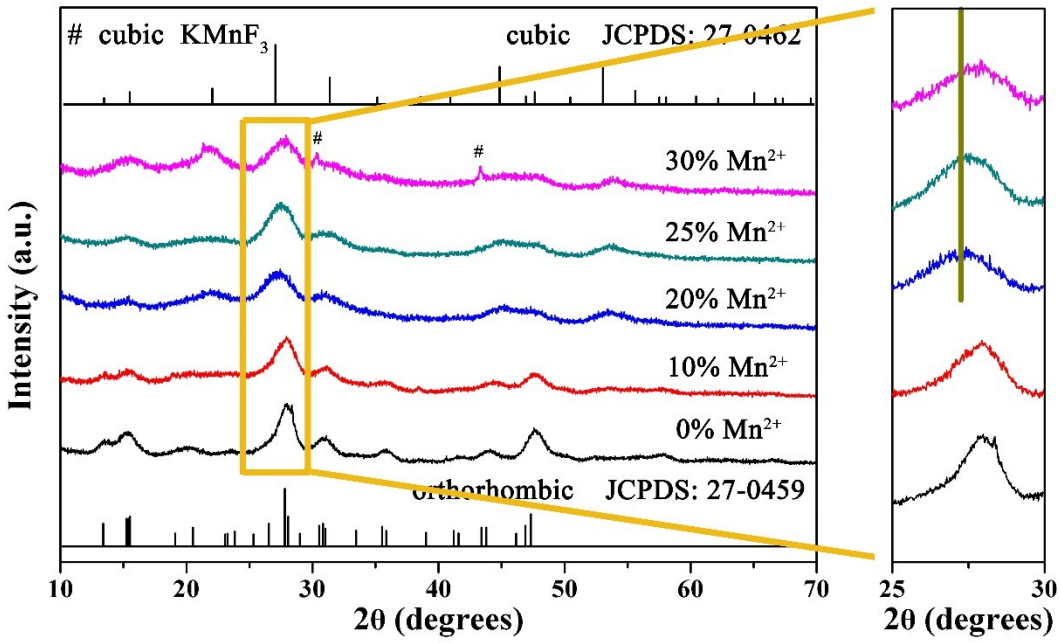

Fig. S1 XRD patterns of KLu_2F_7:Yb^{3+}/Er^{3+} nanoparticles in the presence of 0, 10, 20, 25 and 30% Mn^{2+} dopant ions, respectively (obtained at 260 ^oC). The enlarged area showed that the diffraction peak shifts slightly to the higher-angle side as a result of the crystal unit cell contractive due to the substitution of Lu^{3+} ions by smaller Mn^{2+} ions in the host lattice.

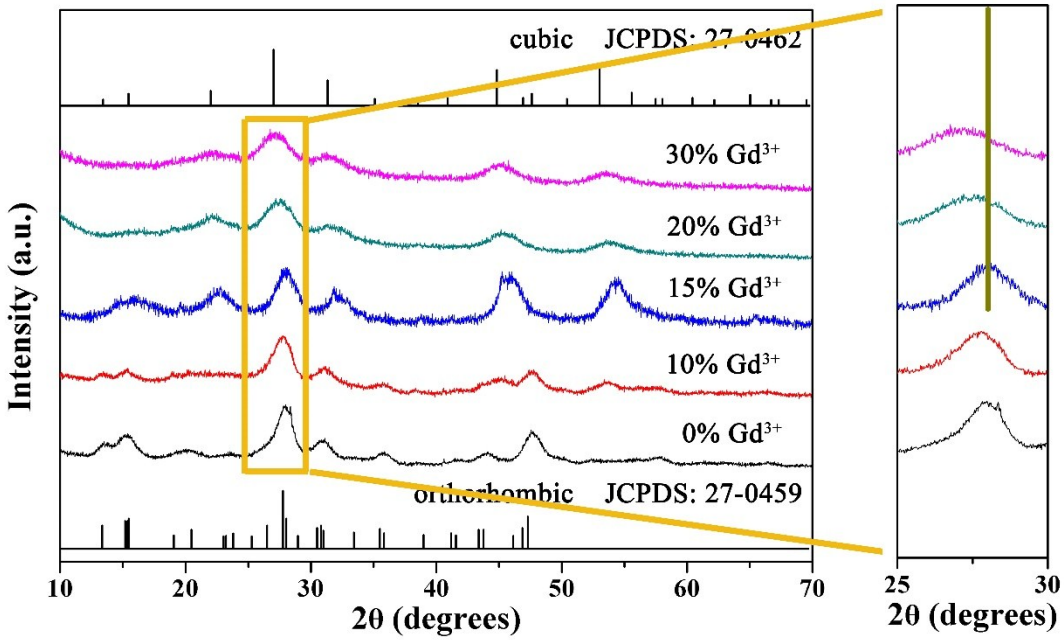

Fig. S2 XRD patterns of KLu_2F_7:Yb^{3+}/Er^{3+} nanoparticles in the presence of 0, 10, 15, 20 and 30% Gd^{3+} dopant ions, respectively (obtained at 260 °C). The enlarged area showed that the diffraction peak shifts slightly to the lower-angle side as a result of the crystal unit cell expanded due to the substitution of Lu^{3+} ions by larger Gd^{3+} ions in the host lattice.

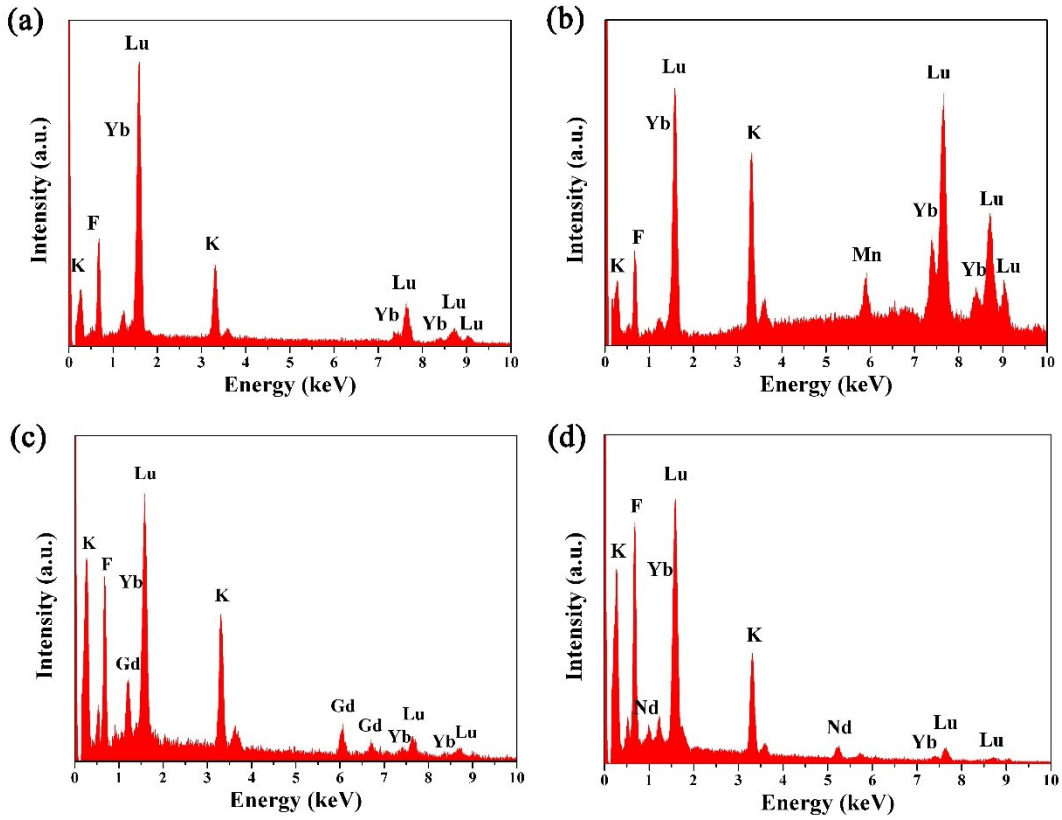

Fig. S3 EDS of the KLu_2F_7:Yb^{3+}/Er^{3+} nanoparticles (a) un-doped and doped with 20% (b) Mn^{2+}, (c) Gd^{3+} and (d) Nd^{3+} ions, respectively (obtained at 260 ^oC).

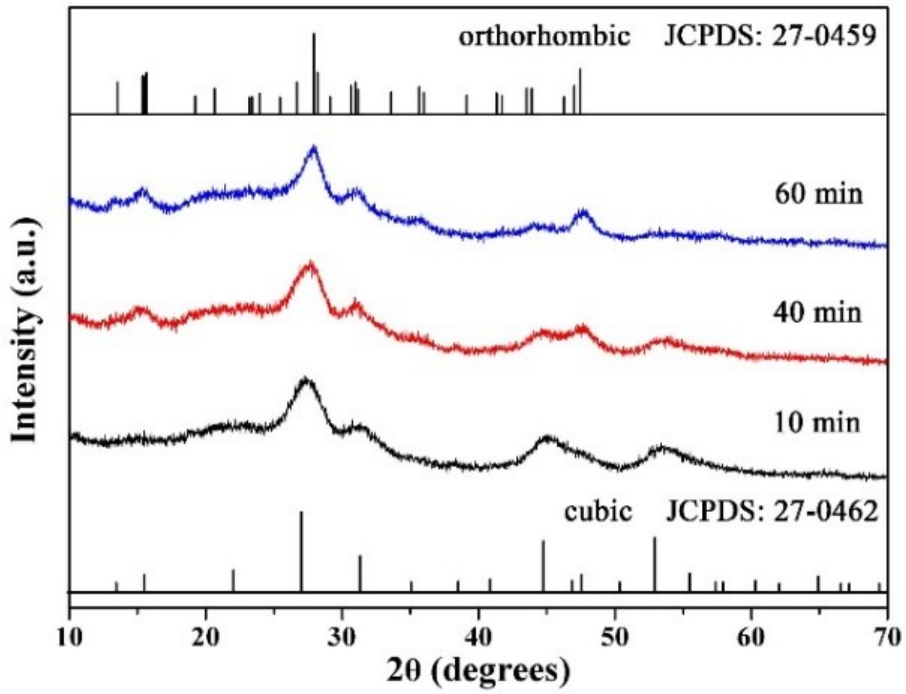

Fig. S4 XRD patterns of KLu_2F_7:Yb^{3+}/Er^{3+} nanoparticles obtained at different reaction times (10 min, 40 min and 60 min) (obtained at 260 ^oC).

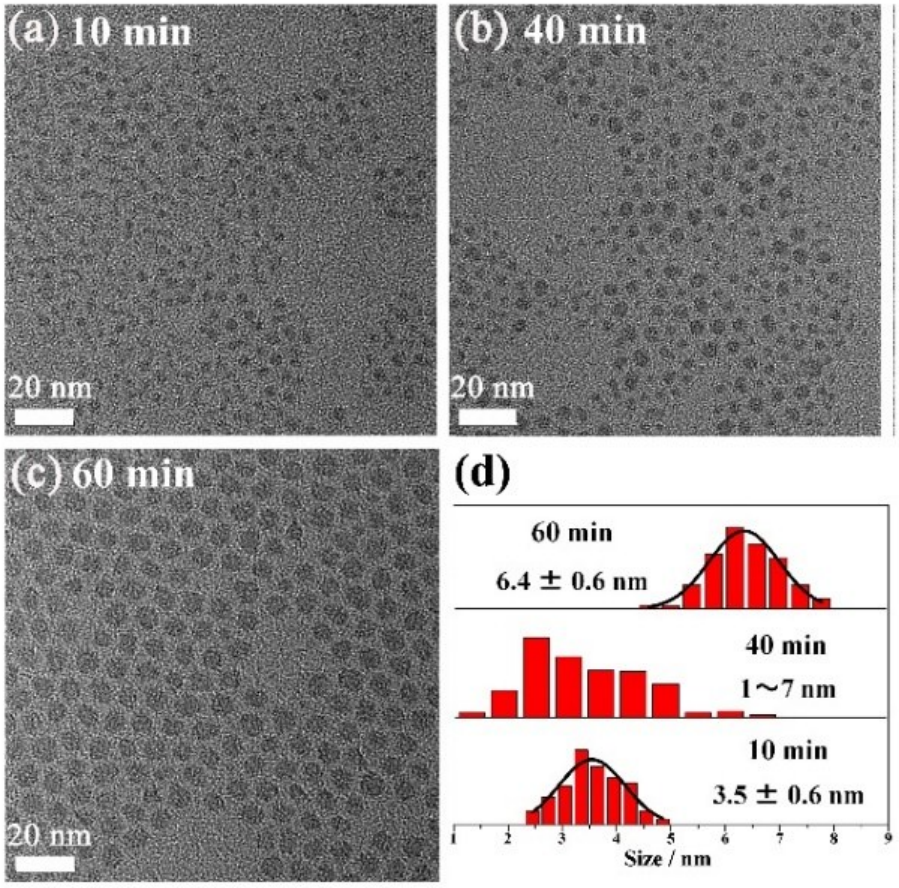

Fig. S5 TEM images of $KLu_2F_7:Yb^{3+}/Er^{3+}$ nanoparticles obtained at different reaction times (a) 10 min, (b) 40 min, (c) 60 min and (d) size distribution of $KLu_2F_7:Yb^{3+}/Er^{3+}$ nanoparticles obtained at different reaction times (obtained at 260 ^{o}C).

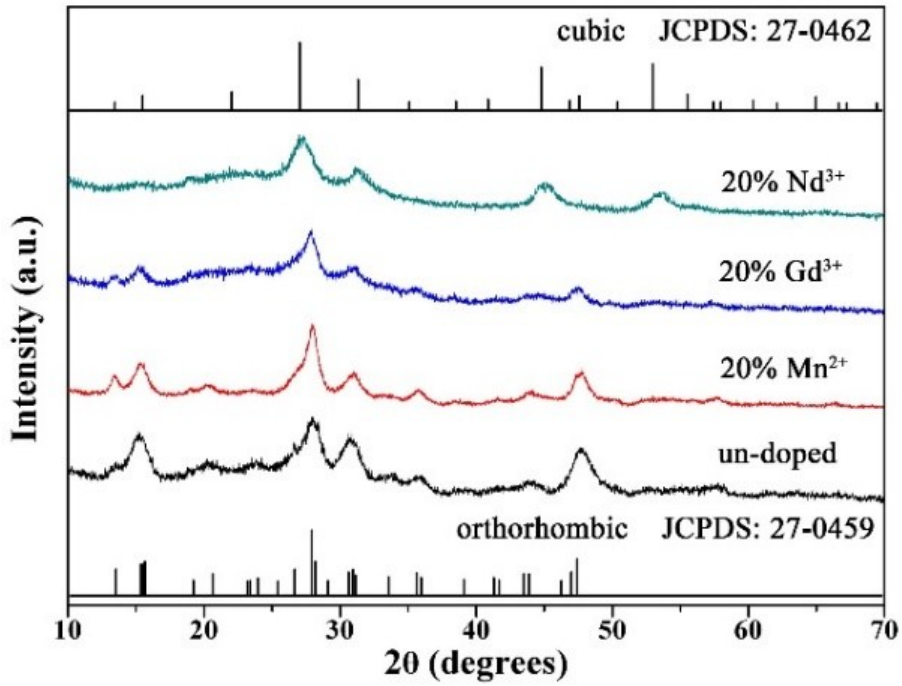

Fig. S6 XRD patterns of $KLu_2F_7:Yb^{3+}/Er^{3+}$ nanoparticles un-doped and doped with 20% Mn^{2+}, Gd^{3+} and Nd^{3+} ions, respectively (obtained at 290 ^oC).

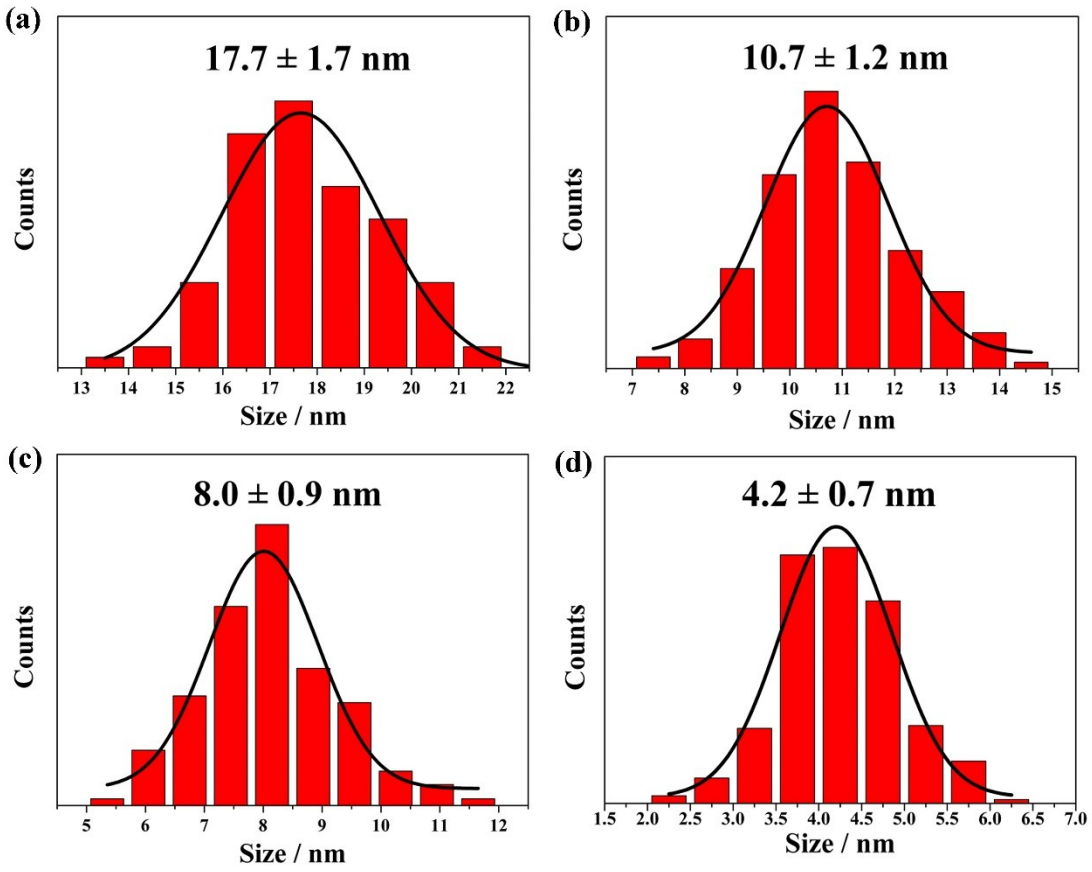

Fig. S7 Size distribution of KLu_2F_7:Yb^{3+}/Er^{3+} nanoparticles (a) un-doped and doped with 20% (b) Mn^{2+}, (c) Gd^{3+} and (d) Nd^{3+} ions, respectively (obtained at 290 ^oC).

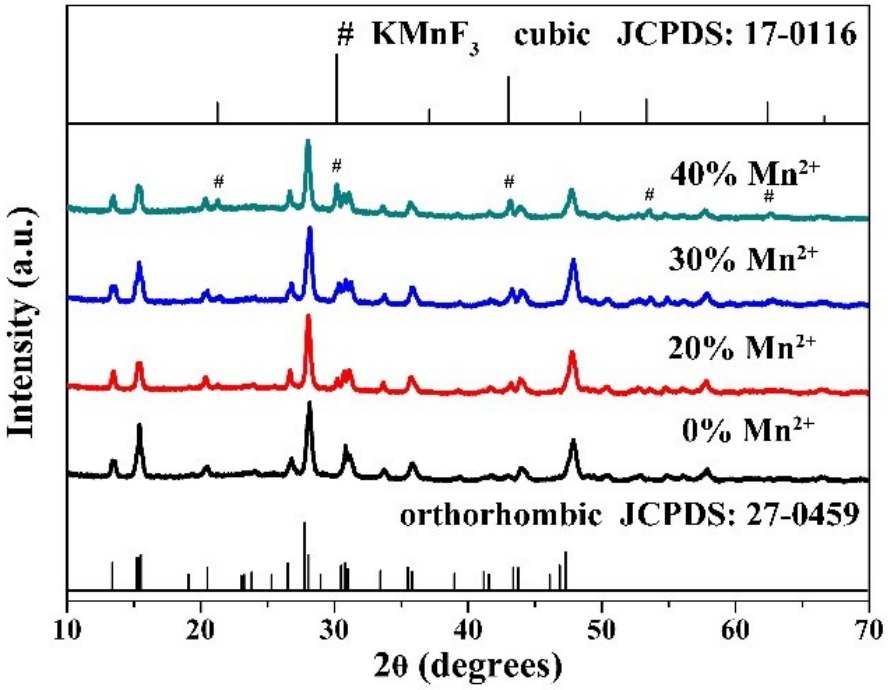

Fig. S8 XRD patterns of KLu_2F_7:Yb^{3+}/Er^{3+} nanoplates in the presence of 0, 20, 30 and 40% Mn^{2+} dopant ions, respectively (obtained at 200 °C).

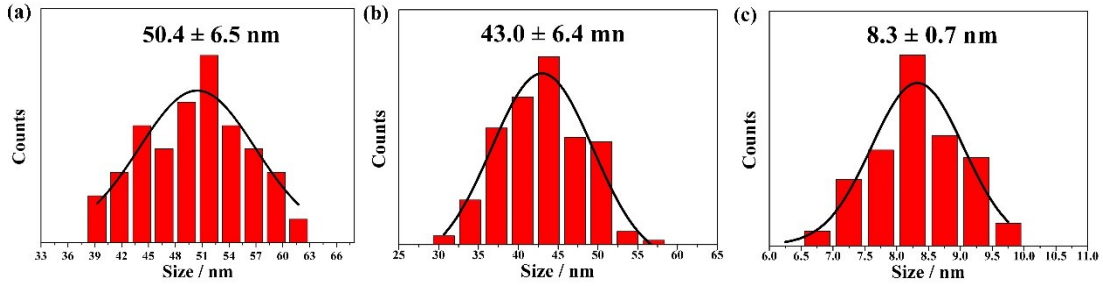

Fig. S9 The size distribution of KLu_2F_7:Yb^{3+}/Er^{3+} nanoparticles (a) un-doped doped with 40% (b) Mn^{2+} and (c) Gd^{3+} ions, respectively (obtained at 200 °C).

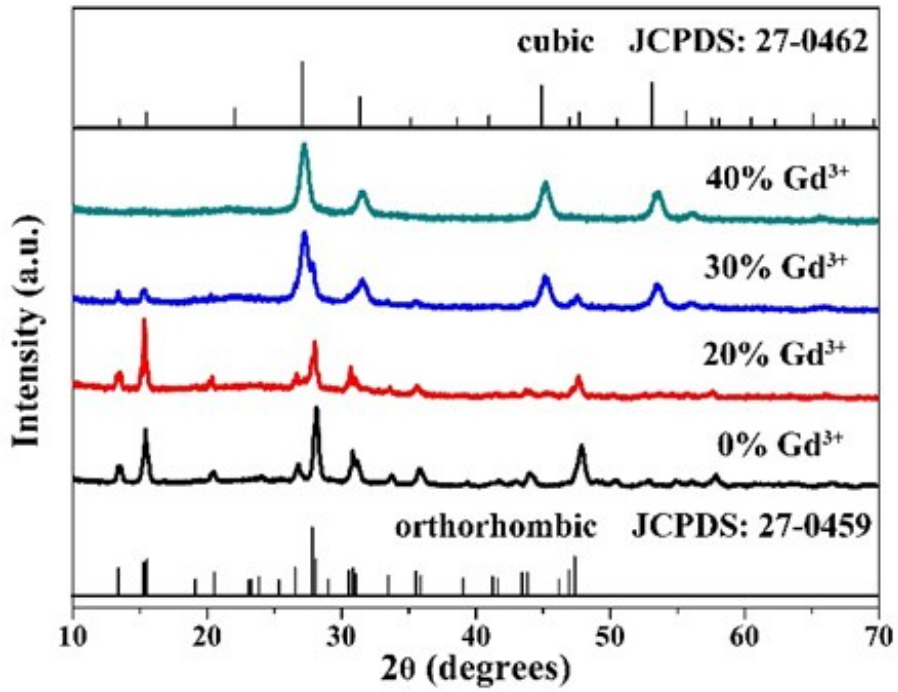

Fig. S10 XRD patterns of KLu_2F_7:Yb^{3+}/Er^{3+} nanoplates in the presence of 0, 20, 30 and 40% Gd^{3+} dopant ions, respectively (obtained at 200 ^oC).

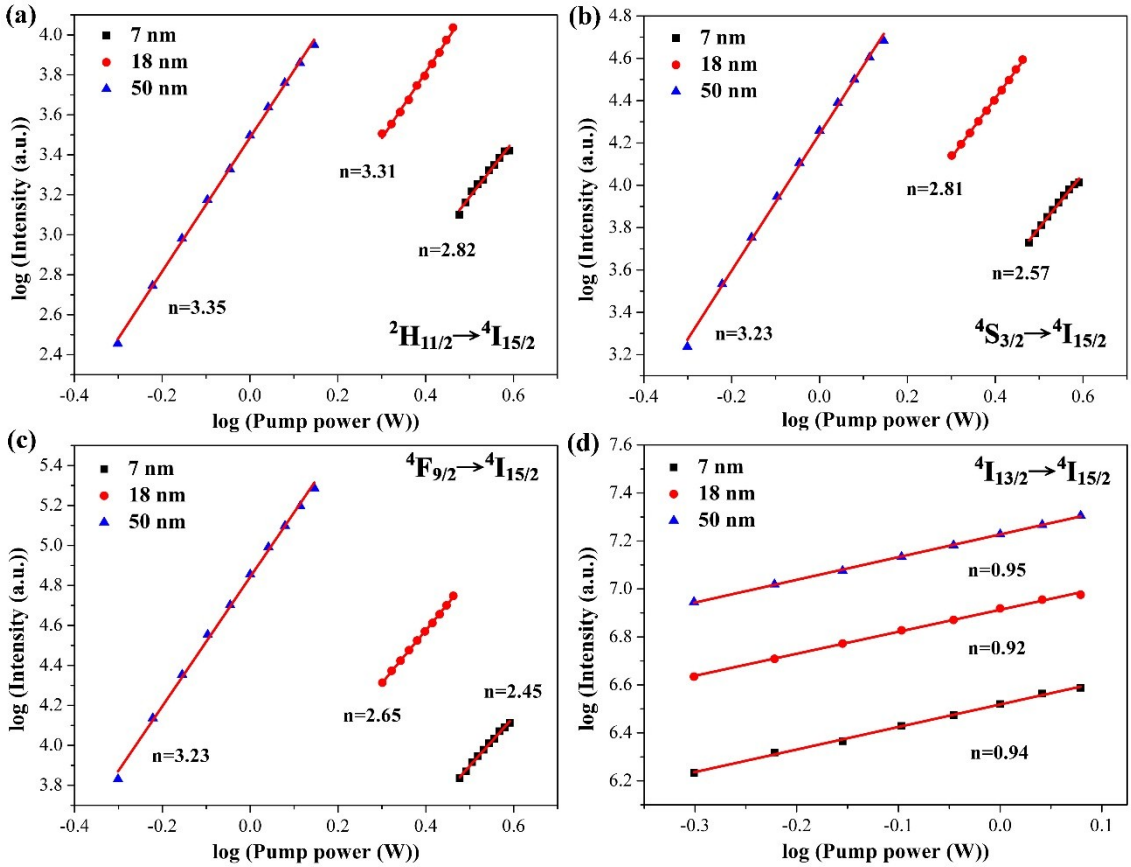

Fig. S11 The double-logarithmic plots of the emission intensity of different transitions of various sized $KLu_2F_7:Yb^{3+}/Er^{3+}$ UCNPs as a function of excitation power, respectively

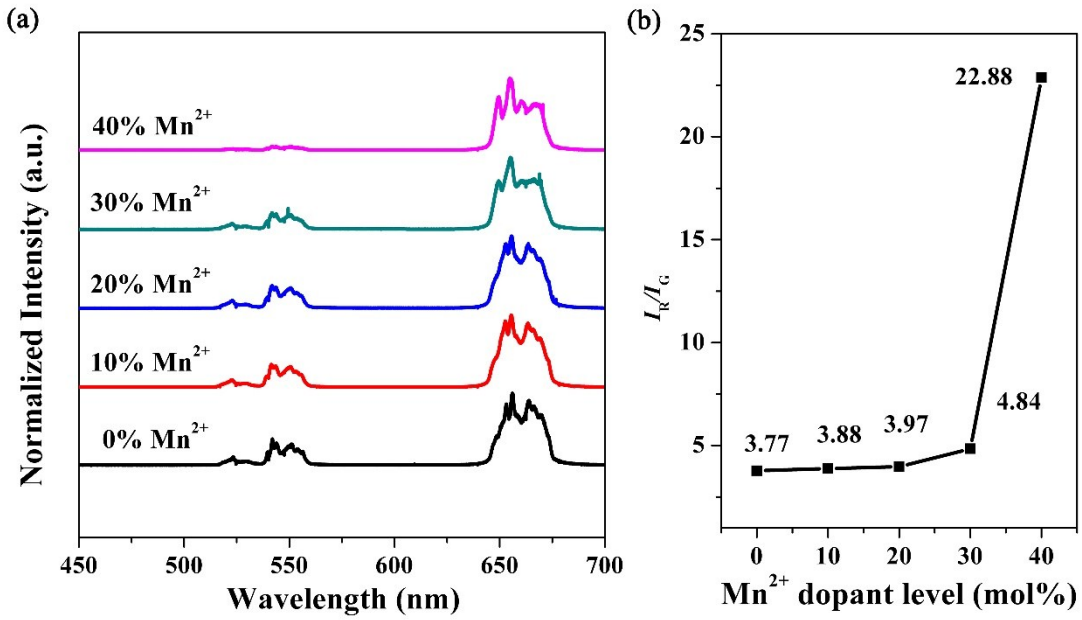

Fig. S12 (a) Normalized upconversion emission spectra of KLu_2F_7:Yb^{3+}/Er^{3+} nanoparticles with different Mn^{2+} ions dopant concentrations. (b) Red to green emission intensity ratio (I_R/I_G) versus dopant concentration of Mn^{2+} ions.